Evaluation of the memory kernel for fluctuation decay in simulated glass-forming $Ni_{0.5}Zr_{0.5}$ liquids

H. Teichler
Institut für Metallphysik, Universität Göttingen, and Sonderforschungsbereich 345, D-37073 Göttingen, Germany
(Received 11 December 1995)

Molecular dynamics simulations for undercooled glass-forming $Ni_{0.5}Zr_{0.5}$ liquids are analyzed to evaluate the memory kernel that governs the decay of structural fluctuations according to the schematic model of the mode coupling theory. The resulting kernel exhibits significant structures which explains the absence of the inverse power law decay in the early β regime. [S1063-651X(96)51005-6]

PACS number(s): 61.20.Ja, 64.70.Pf

The present contribution is concerned with the decay of structural fluctuations in glass-forming, undercooled liquids, especially with the estimation of the underlying memory kernel from molecular dynamics (MD) simulations of the related correlation function. This problem is of particular importance with regard to the liquid-glass transition [1]. According to the seminal papers of Bengtzelius, Götze, and Sjögren [2], and independently of Leutheusser [3], the mode coupling theory (MCT) for dense liquids (e.g. [4,5]) implies that the liquid (''ergodic'') state is characterized through a decay of structural correlations while below a critical temperature T_c a solidlike ''nonergodic'' state with structural arrest exists where fluctuations are effectively frozen. Here correlations decay on a longer time scale by thermally activated diffusion processes [6–8]. All these details are hidden in the memory kernel.

The ''schematic'' model of the MCT proposed in [2,3] predicts the T_c transition and makes detailed predictions (compare, e.g., [9]) about the fluctuation dynamics in the system, like the final α decay and the preceding β regime. The predictions were verified qualitatively and quantitatively in many cases by experiments and MD computer simulations (see, e.g., the compilation in [10]). Also the predictions of the full MCT for the α decay recently were successfully compared with the fluctuation dynamics of colloidal suspensions from light scattering experiments by van Megen and Underwood [11]. Despite this great success in interpreting undercooled liquids' dynamics there are in some cases discrepancies found between the MCT predictions for the early β regime and data from, e.g., MD simulations, like [10,12,13], and experiments, like the recent Raman scattering measurements [14], where in [14] the discrepancies are ascribed to atomic vibrations neglected in the MCT.

The predictions of the schematic MCT model crucially depend on the assumption that the memory kernel which describes the decay of the fluctuations and the dynamics of the corresponding correlation function $\Phi(t)$, can be expressed in the relevant regime as a monotonic and differentiable function of $\Phi(t)$. Our recent analysis [13] of the self-intermediate scattering function in a MD simulated $Ni_{0.5}Zr_{0.5}$ model already revealed that reproduction of the MD data as solutions of the schematic MCT equation demands a more general approach. This raises the question for explicit evaluation of the memory kernel from MD simulated (or experimentally determined) correlation functions to compare with the MCT assumptions, a question so far not considered in the literature, to our knowledge. Such an evaluation is the central point of the present study, where we analyze the MD generated self-intermediate scattering function of the mentioned $Ni_{0.5}Zr_{0.5}$ model.

In our analysis we introduce the memory kernel $F(t)$ via the equation of motion for the correlation function $\Phi(t)$ which according to the MCT can be expressed as a damped harmonic oscillator function

$$\partial_t^2\Phi(t)/\omega_0^2+\Phi(t)+\int_0^t dt' F(t-t')\partial_t\Phi(t')=0 \qquad (1)$$

with initial conditions $\Phi(0)=1$ and $\partial_t\Phi(0)=0$. From the MCT it is known, and was recently reconfirmed by Kawasaki [5], that $F(t)$ for a density fluctuation with wave vector $\mathbf{q}$ involves products of correlation functions of fluctuations with different $\mathbf{q}$, the diffusion coefficient, and the instantaneous viscosity coefficient. The schematic theory proposed in [2,3] models the products of correlation functions by polynomials in the correlator under consideration. The ''idealized schematic theory'' neglects atomic diffusion and relies on the assumption

$$F(t)=F_0(t):=h(t)+f(\Phi(t)), \qquad (2)$$

where $f(\Phi)$ means the polynomial in Φ and $h(t)$ a short time viscous damping which conveniently is approximated by an instantaneous term $\eta_0\delta(t)$. The asymptotic behavior of $\Phi(t)$ is determined by $f(\Phi)$. A decisive role here is played by the quantity introduced in [13]

$$g(\Phi)=f(\Phi)(\Phi^{-1}-1) \qquad (3)$$

with $\Phi\in[0,1]$. $g(\Phi)$ is related in a simple way to $\Delta F(\Phi)=f(\Phi)-\Phi/(1-\Phi)$ frequently used in the schematic MCT (e.g., [15]). If $g(\Phi)<1$ for all $\Phi\in[0,1]$ then the solutions $\Phi(t)$ of Eq. (1) decay to zero and correlations between structural fluctuations vanish at large t. The correlator describes an ergodic liquid. In the following we use $g_m:=\mathrm{Max}\{g(\Phi)\}$, and $\Phi_m\in[0,1]$ the position of the maximum. For $g_m>1$ a structural arrest with $\Phi(t\to\infty)=\Phi_0>0$ may take place where structural fluctuations are effectively frozen. This characterizes the nonergodic low-temperature situation. $g_m=1$ is the critical condition for a change in the fluctuation dynamics and is related to the critical temperature T_c.

The ''extended schematic theory'' simulates atomic diffusion by taking into account the coupling to transverse currents. This yields

$$F(t)=\mathscr{L}^{-1}\{1/[D(z)+1/\mathscr{L}\{F_0(t)\}_z]\}_t. \tag{4}$$

Here $\mathscr{L}$ means the Laplace transform, $\mathscr{L}^{-1}$ its inverse. $D(z)$ models the coupling to the transverse currents. It leads to the final decay of structural fluctuations also below T_c. This sets one of the basic problems in the classification of the solutions of Eq. (1) as it may not be obvious for a given solution whether it belongs to the regime above or below T_c if atomic diffusion is included.

To carry out our analysis we introduce

$$F_c(\omega)+iF_s(\omega)=\lim_{\eta\to 0}\mathscr{L}\{F(t)\}_{\eta-i\omega} \tag{5}$$

[and $\Phi_c(\omega)$, $\Phi_s(\omega)$ analogously] which gives from Eq. (1)

$$\omega F_c(\omega)=\omega\Phi_c(\omega)/R(\omega), \tag{6}$$

$$R(\omega)=[1-\omega\Phi_s(\omega)]^2+[\omega\Phi_c(\omega)]^2, \tag{7}$$

while the time dependent kernel follows from

$$F(t)=(2/\pi)\int_0^\infty d\omega\ F_c(\omega)\cos(\omega t). \tag{8}$$

Below we apply Eqs. (5)–(8) to evaluate from MD simulations for a $Ni_{0.5}Zr_{0.5}$ model the memory kernel for the self-part of the intermediate scattering function

$$\Phi(\mathbf{q},t):=\langle\langle\exp\{i\mathbf{q}\cdot\mathbf{x}_j(t+t_0)-\mathbf{x}_j(t_0)]\}\rangle\rangle. \tag{9}$$

The brackets mean averages over the atoms j and the initial configurations t_0.

The MD simulations are carried out as state-of-the-art isothermal-isobaric (N,t,p) calculations. The Newtonian equations of $N=648$ atoms are numerically integrated by a fifth order predictor-corrector algorithm (time step $\Delta t=2.5\times10^{-15}$ s) in a cubic volume with periodic boundary conditions and variable box length L. The interatomic couplings are modeled as in [13,16] by a volume dependent electron-gas term $E_{\rm vol}(V)$ and pair potentials $\phi(r)$ adapted to the equilibrium distance, depth, width, and zero of the electron-theoretical Hausleitner-Hafner potentials [17] for $Ni_{0.5}Zr_{0.5}$. In the present study we concentrate on $\mathbf{q}$ values of 21.8 nm^{-1} lengths parallel to the edges of the simulation cube, which correspond to wavelengths of approximately the averaged nearest neighbor distance.

In [13] a value of $T_c\approx1120$ K was estimated for this model. Here we consider configurations around this T_c. Those for 1100 K and above are generated by ''cooling'' the system in the computer from 3000 K with rate $-\partial T=2.5\times10^{12}$ K/s to the desired temperature and afterwards equilibrating it isothermally during additional 10^6 integration steps (nominally 2.5 ns). The further evolution of these relaxed configurations then is studied. To model with sufficient statistical significance the short time behavior below 90 ps we use 16 randomly selected configurations along the latter evolution path as initial configurations for simulation runs. The short time $\Phi(\mathbf{q},t)$ are averages over these runs. The long time data present averages over the full evolution paths. For generating the 1040 and 980 K structures the isothermally equilibrated 1100 K configuration was cooled further down with a rate of 2.75×10^9 K/s (i.e., 17.2×10^6 additional integration steps to obtain the 980 K structure) followed by 5 ns, respectively, 10 ns MD production runs. Due to this processing the low-temperature data describe much better relaxed structures than studied in [13].

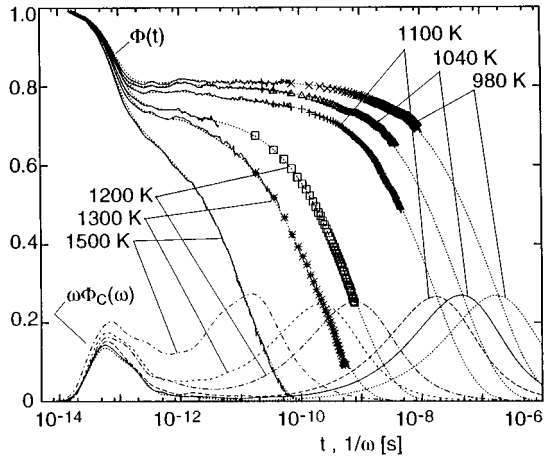

FIG. 1. Self-intermediate scattering function $\Phi(T)$ from MD simulations for $Ni_{0.5}Zr_{0.5}$ (wiggly lines: short time data; symbols: long time data; dotted lines: smoothed curves with extrapolation) and susceptibility $\omega\Phi_c(\omega)$ of the smoothed curves.

Figure 1 provides our results for the self-part of the intermediate scattering function, Eq. (9), in a time window between 10^{-14} and 10^{-8} s. It displays by wiggly lines the short time results while the symbols give the long time behavior. Where necessary the curves are extrapolated by assuming an asymptotic stretched exponential behavior $\phi_0\exp[-(t/\tau)^\beta]$ with common value $\beta=0.65(4)$ for all temperatures. (This choice of β shall be justified later.) From these ''raw'' data smoothed curves are generated and provided in Fig. 1 by dotted lines. In Fig. 1 also are shown the related susceptibilities $\omega\Phi_c(\omega)$.

The spectral distributions $\omega F_c(\omega)$ deduced via Eq. (6) from $\omega\Phi_c(\omega)$ and $\omega\Phi_s(\omega)$ (the latter is not shown in Fig. 1 for clearness of the presentation) are displayed in Fig. 2 as well as the corresponding $F(t)$. Evaluation of $\omega F_c(\omega)$ for high frequencies at the upper limit of the vibrational peak deserves some care since minor, spurious intensities in $\omega\Phi_c(\omega)$ may give rise to enormously enhanced structures in $\omega F_c(\omega)$ due to $\omega\Phi_s(\omega)\to1$ in this frequency regime. In the smoothing process we have tried to eliminate unrealistic high-frequency fluctuations. Nevertheless, there remains some uncertainty in $\omega F_c(\omega)$ at high ω, respectively in $F(t)$ at small t, which may explain the deviations from a strictly monotonic temperature dependence in the mentioned regimes.

Obviously the obtained $F(t)$ can be cast into the form of Eq. (2), which means the dynamics of the system can be mapped onto those of an idealized schematic one. In Fig. 3(a) we tentatively plot $F(t)$ vs $\Phi(t)$, i.e., $F(\Phi)$. According to this plot there exist limiting values $\Phi_0(T)$ so that $F(\Phi)$ for $\Phi<\Phi_0(T)$ is close to a universal behavior while for

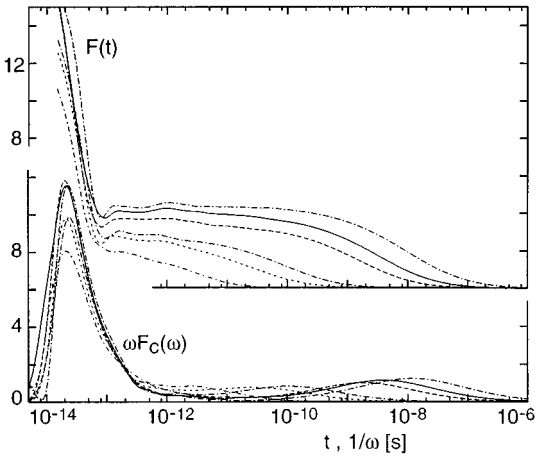

FIG. 2. Memory kernel $F(t)$ (upper part) related to the self-intermediate scattering function and spectral distribution $\omega F_c(\omega)$ for the kernel (lower part). (Temperatures as in Fig. 1).

$\Phi > \Phi_0(T)$ deviations are seen. $\Phi_0(T)$ significantly decreases with increasing T. It is tempting to model $F(\Phi)$ below $\Phi_0(T)$ by a (weakly T-dependent) polynomial $P(\Phi)$, consider this polynomial as a representation of $f(\Phi)$, and extend it to $\Phi > \Phi_0(T)$. According to Eq. (2) a suitable $h(t)$ then can be introduced as the difference between $F(t)$ and $P(\Phi(t))$. For the present model the $h(t)$ are limited to times below 3 ps due to construction. Figure 3(a) also includes by the dotted line the polynomial $P(\Phi)$ for 980 K. The $P(\Phi)$ for other temperatures are similar but are suppressed for clearness of the presentation. Their coefficients are provided by Table I.

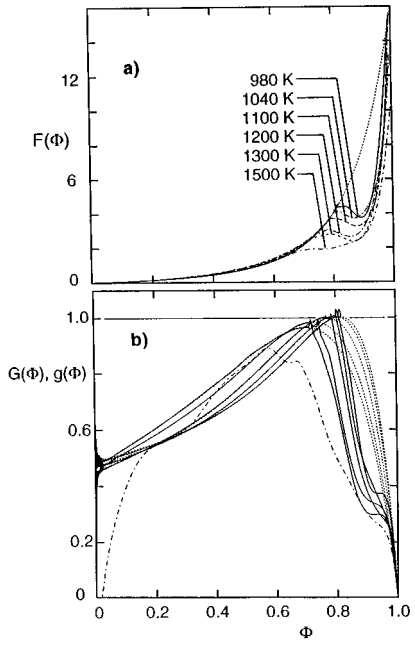

FIG. 3. (a) Memory kernel F as a function of Φ (dotted line: extrapolated low-Φ polynomial at 980 K). (b) $G(\Phi)$ (full lines) and $g(\Phi)$ (dotted lines) according to Eqs. (10) and (11). [Dash-dotted line: $G(\Phi)$ at 1500 K.]

TABLE I. Coefficients of the polynomial expansion $f(\Phi) = \Sigma_n \lambda_n \Phi^n$.

	980 K	1040 K	1100 K	1200 K	1300 K
n			λ_n		
1	0.4834	0.4660	0.4215	0.4510	0.4660
2	0.8649	0.8986	1.2019	1.1942	1.2346
3	0.2442	0.2390	0.1472	0.2735	0.3920
4	2.9165	3.0881	2.5615	3.3390	3.4695
5	0.1073	0.1359	0.1486	0.1919	0.1373
6	1.2762	1.5720	2.2363	1.8626	1.3054
7	2.4758	2.9143	5.0374	2.8314	2.0658
8	0.0031	0.0032	0.0072	0.0019	0.0018
9	0.9067	0.7618	0.2298	0.0288	0.0368
10	6.8123	4.7400	0.3077	0.0196	0.0323

For our final discussion we present in Fig. 3(b) the quantities

$$G(\Phi) := F(\Phi)(\Phi^{-1} - 1), \tag{10}$$

$$g(\Phi) = P(\Phi)(\Phi^{-1} - 1), \tag{11}$$

i.e., the analog to Eq. (3), where $f(\Phi)$ in $g(\Phi)$ now is substituted by $P(\Phi)$. The $G(\Phi)$'s have a more pronounced T dependence than the $F(\Phi)$. [Therefore we have determined $P(F)$ as the polynomial with non-negative coefficients which fits best $g(\Phi)$ to $G(\Phi)$ for $\Phi < \Phi_0(T)$.] The 1500 K curve strikingly differs from the others at low Φ. It indicates deviations from the stretched exponential behavior which may be attributed to isolated decay events.

The $g(\Phi)$ are displayed in Fig. 3(b) by dotted lines. They remain below the critical value one—or touch it in a region where $h(t)$ is active—while the overshooting of $G(\Phi)$ over this limit is included in $h(t)$. The $g(\Phi)$ show maxima with $g_m < 1$ for $T \geqslant 1200$ K and $g_m \approx 1$ for $T = 1100, 1040, 980$ K. This reconfirms our earlier conclusion [13] that the system is in the liquid, ergodic state at 1200 K and above. The behavior at 1100 K and below may be interpreted as ''nearly arrested'' with correlation decay due to thermally excited atomic diffusion, in agreement with [13] and $T_c \approx 1200$ K estimated there. Here we now may comment on the value of the stretched exponential parameter β used to extrapolate the MD data into the late α regime. The idealized schematic theory (e.g., [15]) predicts that the dynamics around T_c are governed by the exponential parameter $\lambda = (1-\Phi)^3[\partial^2 f(\Phi)/\partial \Phi^2]/2$ (at $\Phi = \Phi_m$ for $T \approx T_c$). From our 1100 K curve in the range of the MD data with $f(\Phi) = P(\Phi)$ a value $\lambda = 0.65(3)$ follows. Therefrom, by $\beta = -\ln(2)/\ln(1-\lambda)$ [7], we get $\beta = 0.65(4)$ as used in the extrapolation.

The presentation in Fig. 3 offers a straightforward interpretation of the decay scenery. The system behaves like an idealized schematic one governed by two different decay processes. As is typical for the (schematic) MCT the long time process has a time scale set by the fluctuations under consideration, i.e., $f(t) = P(\Phi(t))$. The short time process, characterized by $h(t)$, has a time scale set by an independent

mechanism. $h(t)$ is active in the time range where the atomic motion is governed by the vibrations in local cages. Hence it seems justified to ascribe $h(t)$ to these vibrations and to interpret its effect as randomization of the structure due to (nonlinearities in) this motion. Below and around T_c the combined action of both processes carries the system to a temporary structural arrest at $\Phi_m \cdot \Phi_0(T)$ indicates the crossover from the combined action of both processes to the action of the pure long-time process. Φ_m and $\Phi_0(T)$ nearly coincide since Φ_m is more or less reached before $h(t)$ gets ineffective and the system remains at this value a sufficient long time for $h(t)$ to die out.

Now we are in the position to address the initial question concerning the behavior of $\Phi(t)$ in the early β regime, i.e., the regime with $\Phi(t)$ slightly above Φ_m. For this regime the schematic theory with instantaneous viscous damping deduces from the polynomial approach for $f(\Phi)$ an inverse power-law decay $\partial_t \Phi - t^{-(a+1)}$ [9] where the parameter a is related to the exponential parameter λ. Our analysis shows that around T_c in this Φ range the structural decay is markedly determined by $h(t)$ which masks this power law. It is the particular fact that $\Phi_m(T)$ and $\Phi_0(T)$ nearly coincide which yields that the inverse power law is not visible in the correlation function. Consequently there is no β peak detectable apart from the vibrations while the later part of the β regime is well developed as here $h(t)$ already died out. Our point of view agrees with the interpretation by Rössler *et al.* [14], who from experimental observations attribute the suppression of the inverse power law to the atomic vibrations. While our treatment greatly reconfirms for lower Φ the MCT assumption of a smooth and weakly T-dependent $f(\Phi)$ it reveals significant deviations at larger Φ which emphasizes the need for incorporation of atomic vibrations in the microscopic MCT.

[1] J. Jäckle, Rep. Prog. Phys. **49**, 171 (1986).
[2] U. Bengtzelius, W. Götze, and A. Sjölander, J. Phys. C **17**, 5915 (1984).
[3] E. Leutheusser, Phys. Rev. A **29**, 2765 (1984).
[4] K. Kawasaki, Phys. Rev. **150**, 291 (1966); Ann. Phys. (N.Y.) **61**, 1 (1970).
[5] K. Kawasaki, Physica A **208**, 35 (1994).
[6] P. S. Das and G. F. Mazenko, Phys. Rev. A **34**, 2265 (1986).
[7] W. Götze and L. Sjögren, J. Phys. C **21**, 3407 (1988).
[8] L. Sjögren, Z. Phys. B **79**, 5 (1990).
[9] W. Götze and L. Sjögren, Rep. Prog. Phys. **55**, 241 (1992).
[10] W. Kob and H. C. Andersen, Phys. Rev. E **51**, 4626 (1995).
[11] W. van Megen and S. M. Underwood, Phys. Rev. E **49**, 4206 (1994).
[12] L. J. Lewis and G. Wahnström, Phys. Rev. E **50**, 3865 (1994); L. J. Lewis, Mat. Sci. Eng. A **133**, 423 (1991); G. Wahnström, Phys. Rev. A **44**, 3752 (1991).
[13] H. Teichler, Phys. Rev. Lett. **76**, 62 (1996).
[14] E. Rössler, A. P. Sokolov, A. Kisliuk, and D. Quitmann, Phys. Rev. B **49**, 14 967 (1994).
[15] W. Götze and R. Haussmann, Z. Phys. B **72**, 403 (1988).
[16] H. Teichler, Phys. Status Solidi B **172**, 325 (1992).
[17] Ch. Hausleitner and J. Hafner, Phys. Rev. B **45**, 128 (1992).